separations

MDPI

Article

A Novel Fixed-Bed Process Integrated with Additional Disproportionation Reactors for Silane Production

Qiang Geng [1,2,†], Tianshi Lan [1,3,†] and Guoqiang Huang [1,2,*]

[1] School of Chemical Engineering and Technology, Tianjin University, Tianjin 300072, China; 2019207415@tju.edu.cn (Q.G.); 1124207008@tju.edu.cn (T.L.)
[2] State Key Laboratory of Chemical Engineering and Low-Carbon Technology, Tianjin 300072, China
[3] GCL Technology Holdings Limited, Hong Kong, China
* Correspondence: hgq@tju.edu.cn
† These authors contributed equally to this work.

Abstract

With the increase in the demand for electronic-grade high-purity silane in the semiconductor chip industry, it is of great significance to develop a green and economical method for silane production. Therefore, a novel energy-saving fixed-bed process was proposed innovatively. In this paper, the thermodynamics and kinetics of the trichlorosilane disproportionation system were studied, and the optimal reaction conditions for the resin catalyst were determined, which were used for the subsequent simulation. Based on the conventional DR1 + DR2 process (which includes one trichlorosilane disproportionation reactor (DR1) and one dichlorosilane disproportionation reactor (DR2)), by adding an additional disproportionation reactor to the TCS recycle loop and/or DCS recycle loop, three improved process configurations were designed, including 2DR1 + DR2, DR1 + 2DR2, and 2DR1 + 2DR2 processes. Then, combined with four-column heat integration, the HI + 2DR1 + 2DR2 process was proposed to solve the bottleneck problems of high energy consumption and large circulation flow rate. The results show that the HI + 2DR1 + 2DR2 process achieved the best energy-saving effect. The TCS recycle loop flow rate reduced by 36.87%, the DCS recycle loop flow rate reduced by 12.41%, total energy consumption decreased by 62.8%, and CO_2 emissions decreased by 56.72%. The unit energy consumption is 13.8 kg steam/kg SiH_4, and the silane purity is greater than 99.9999%. This design can be easily applied to the existing production process of the silane plant, achieving energy-saving and low-cost production of silane.

Keywords: trichlorosilane; disproportionation; silane; energy-saving; process intensification

Check for updates

Academic Editor: Yundong Wang

Received: 12 March 2026
Revised: 9 April 2026
Accepted: 16 April 2026
Published: 21 April 2026

Copyright: © 2026 by the authors. Licensee MDPI, Basel, Switzerland. This article is an open access article distributed under the terms and conditions of the Creative Commons Attribution (CC BY) license.

1. Introduction

Silane (SiH_4) is a very important inorganic compound and an indispensable basic chemical raw material in modern high-tech industries and advanced materials fields. Its application scope is still expanding. As a high-purity silicon source gas, it is crucial in semiconductor, photovoltaic, and display film deposition processes [1,2]. With the increasing demand for energy density in the lithium battery industry, traditional graphite negative electrode materials have approached their performance limits. Silicon-carbon negative electrode materials [3] are considered the next generation mainstream negative electrode material by the market due to their high capacity and low cost. The nano-silicon particles formed by the thermal decomposition of silane are the core of the new silicon-carbon technology. Therefore, the demand for silane worldwide has been increasing year by year. The

traditional improved Siemens process [4,5] uses pure trichlorosilane as the raw material, which is cracked in a chemical vapor deposition reactor at 1373 K and then deposited on a silicon mandrel to obtain rod-shaped silicon. The conversion rate of this process is approximately 12%. In contrast, using silane as the raw material, it is decomposed in a fluidized bed reactor at 773 K–973 K and then deposited on a silicon seed to obtain granular silicon, with a conversion rate of up to 98%. The silane method for producing polysilicon is more energy-efficient and is being adopted by more and more production enterprises. The synthesis method of silane has also undergone continuous iterations and developments. The SunEdison Company in the United States used sodium aluminum hydride ($NaAlH_4$) or lithium aluminum hydride ($LiAlH_4$) to reduce silicon tetrafluoride (SiF_4) to produce silane [6], with fluorine salts ($NaAlF_4$) as by-products. The Japanese Mitsui Toatsu Company [7] obtained silane by reacting silicon-magnesium (Si, Mg) alloy with hydrogen chloride (HCl) and hydrogen (H_2) in liquid ammonia (NH_3) and simultaneously generating ammonium chloride (NH_4Cl) and magnesium chloride ($MgCl_2$). These two methods require complex raw materials and produce a large amount of by-products. Therefore, the trichlorosilane disproportionation technology developed by Union Carbide Corporation [8] for preparing silane has become the mainstream process. Trichlorosilane ($SiHCl_3$) can be synthesized through the hydrogenation reaction of silicon tetrachloride ($SiCl_4$) or the chlorination-hydrogenation reaction of metallic silicon. Then, under the catalytic condition of quaternary ammonium ion exchange resin, trichlorosilane disproportionates to dichlorosilane (SiH_2Cl_2), and dichlorosilane disproportionates to silane. The by-product, silicon tetrachloride, can be recycled through the hydrogenation reaction.

The catalyst for the disproportionation reaction of trichlorosilane is usually a quaternary ammonium ion resin based on the polymer of styrene-divinylbenzene as the framework, which has poor high-temperature resistance and is prone to skeleton collapse at high temperatures. Vorotyntsev [9] studied the catalytic performance of Amberlyst A-21 anion exchange resin for the gas-phase disproportionation reaction of trichlorosilane. A three-month test was conducted at a temperature of 423 K, and the reaction results showed that the A-21 resin had stable catalytic activity. The disproportionation reaction of trichlorosilane can be carried out in a fixed-bed reactor or a reactive distillation column. Sun [10] completed the simulation of the reactive distillation process in a dual-column configuration and obtained silane with a purity of 99.9%. Huang [11] reported that setting multiple reaction sections in the reactive distillation column can significantly improve the steady-state performance of the distillation column when converting trichlorosilane into silane. Lee's research [12] found that installing one or two intermediate condensers between the trays of a reactive distillation column can reduce energy costs. However, compared to the widely studied reactive distillation process, the research on the process of preparing silane using a fixed-bed system is relatively scarce. Huang [13] conducted a study on the disproportionation reaction of trichlorosilane to dichlorosilane using the DOWEXMWA-1 resin catalyst in a fixed-bed reactor. The analysis of kinetic data indicated that the reaction was a second-order reaction. The Union Carbide Corporation first reported the process of producing polycrystalline silicon using the fixed-bed silane method [14], as shown in Figure 1; however, at that time, this process was only limited to small-scale laboratory trials. Despite the early commercial success of the UCC process, the high equipment investment and operational costs were largely due to the large mass flow rates of the TCS recycle loop and DCS recycle loop. The unit production cost of silane remains high, and it has no advantage in the current market competition. And there are still no relevant reports on the modeling and optimization of the fixed-bed silane process.

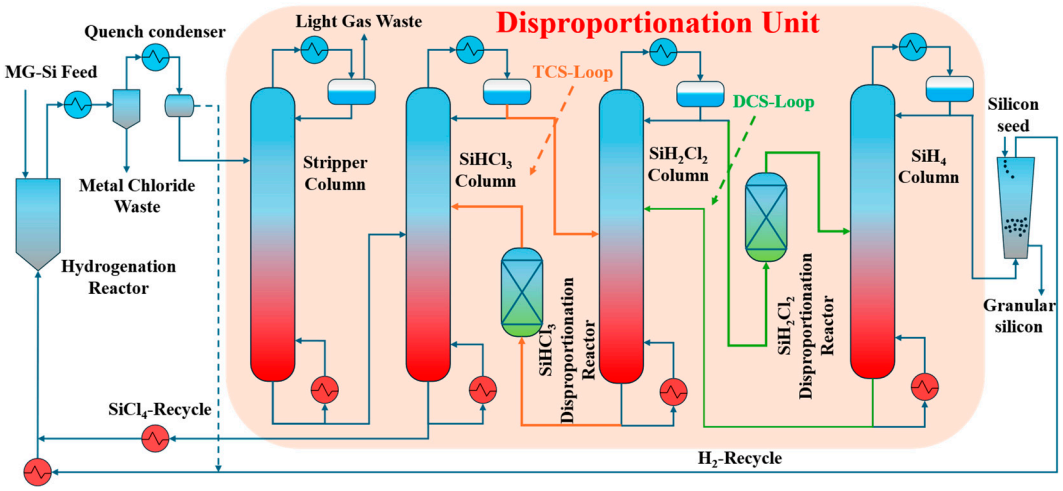


Figure 1. Union Carbide process for polysilicon process.

Therefore, the aim of this study is to design an energy-efficient fixed-bed process that uses the mixed chlorosilane from the cold hydrogenation unit as the raw material, more closely matching the actual industrial production conditions. Firstly, based on thermodynamic analysis and kinetic experimental data, a kinetic model for the catalytic disproportionation reaction of trichlorosilane and dichlorosilane by D301 resin was established. Next, the traditional DR1 + DR2 process for the disproportionation unit, as shown in Figure 1, was designed using Aspen Plus® V11, including a TCS disproportionation reactor and a DCS disproportionation reactor. With the lowest annual total cost as the objective function, the process parameters were optimized using the sequential iterative optimization method. Then, by adding additional disproportionation reactors in the TCS circulation loop and/or the DCS circulation loop, various innovative fixed-bed processes were proposed, including 2DR1 + DR2, DR1 + 2DR2, and 2DR1 + 2DR2 processes. Combined with the four-column heat integration scheme, the HI + 2DR1 + 2DR2 process was designed to minimize the steam consumption per ton of silane. Finally, the total duty, circulation loop flow, and CO_2 emissions of these processes were compared. This work contributes to the existing literature by designing and developing advanced fixed-bed silane processes. These processes aim to reduce the cost of silane production.

2. Modeling and Experiment

2.1. Reaction Equations and Process

The process of synthesizing SiH_4 from $SiHCl_3$ involves three steps of disproportionation reactions, which can be described by the following chemical reaction Equations (1)–(3):

$$2SiHCl_3 \rightleftarrows SiH_2Cl_2 + SiCl_4, R1 \quad (1)$$

$$2SiH_2Cl_2 \rightleftarrows SiH_3Cl + SiHCl_3, R2 \quad (2)$$

$$2SiH_3Cl \rightleftarrows SiH_4 + SiH_2Cl_2, R3 \quad (3)$$

The disproportionation reaction consists of three consecutive reactions, R1–R3. $SiHCl_3$ is first disproportionated to SiH_2Cl_2, then SiH_2Cl_2 is disproportionated to SiH_3Cl, and finally SiH_3Cl is disproportionated to SiH_4. The reaction systems involve five components: $SiCl_4$ (STC), $SiHCl_3$ (TCS), SiH_2Cl_2 (DCS), SiH_3Cl (MCS), and SiH_4 (MS). Their molecular weights and boiling points (101.325 kPa) are shown in Supplementary Material Table S1.

2.2. Thermodynamic Properties

2.2.1. Property Method

An accurate property method plays a crucial role in ensuring the authenticity of the final simulation results. A detailed study on the thermodynamic behavior of the STC-TCS system [15] was conducted in our previous work. Among various methods, the Peng–Robinson state equation [16] fits the gas–liquid equilibrium data of the system well within the minimum deviation range. Therefore, the Peng–Robinson equation of state was selected for the analysis of the chlorosilane (Si-H-Cl) system [17] without azeotropes in this paper.

2.2.2. Thermodynamic Analysis of Reactions

The relevant thermodynamic parameters of the five components involved in the reaction system obtained from the NIST [18] Chemical Handbook are listed in Supplementary Material Table S2. The reaction enthalpy, reaction entropy, reaction Gibbs free energy, and equilibrium constant were calculated according to Formulas (S1)–(S9) in the Supplementary Material, as shown in Figure 2.

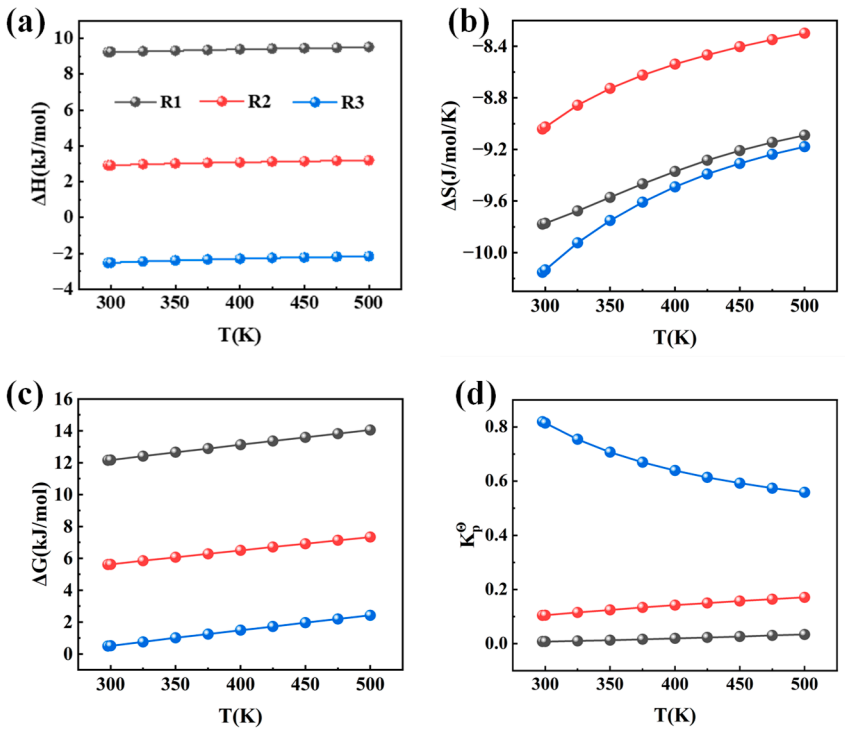


Figure 2. R1–R3: (**a**) reaction enthalpy, (**b**) reaction entropy, (**c**) reaction Gibbs free energy, and (**d**) equilibrium constant.

As shown in Figure 2a, within the temperature range of 300 K–500 K, the reaction enthalpy values of reactions R1–R2 are positive, which demonstrates that the disproportionation of TCS and DCS is an endothermic reaction. The reaction enthalpy value of reaction R3 is negative, indicating that the disproportionation of MCS is an exothermic reaction. From Figure 2b, the entropy values of these three reactions are all negative. Additionally, it was observed that the entropy values gradually increased with rising reaction temperature. Figure 2c shows that the reaction Gibbs free energy values of reactions R1–R3 are all positive, making it difficult for the disproportionation reaction to proceed spontaneously. Among them, the spontaneous disproportionation of TCS is the most difficult. It can be seen from Figure 2d that the reaction equilibrium constants of R1 and R2 both rise with the increase in reaction temperature, while the reaction equilibrium constant of R3 decreases

with the increasing reaction temperature. Therefore, it can be concluded that the increase in temperature promotes the disproportionation of TCS and DCS thermodynamically but inhibits the conversion of MCS to MS.

The equilibrium product distribution of pure TCS, DCS, and MCS as reactants was studied in a Gibbs reactor based on the Gibbs free energy minimization method. The variation trends of the mole fractions of the five components and the conversion rates of reactants with temperature are displayed in Figure 3.

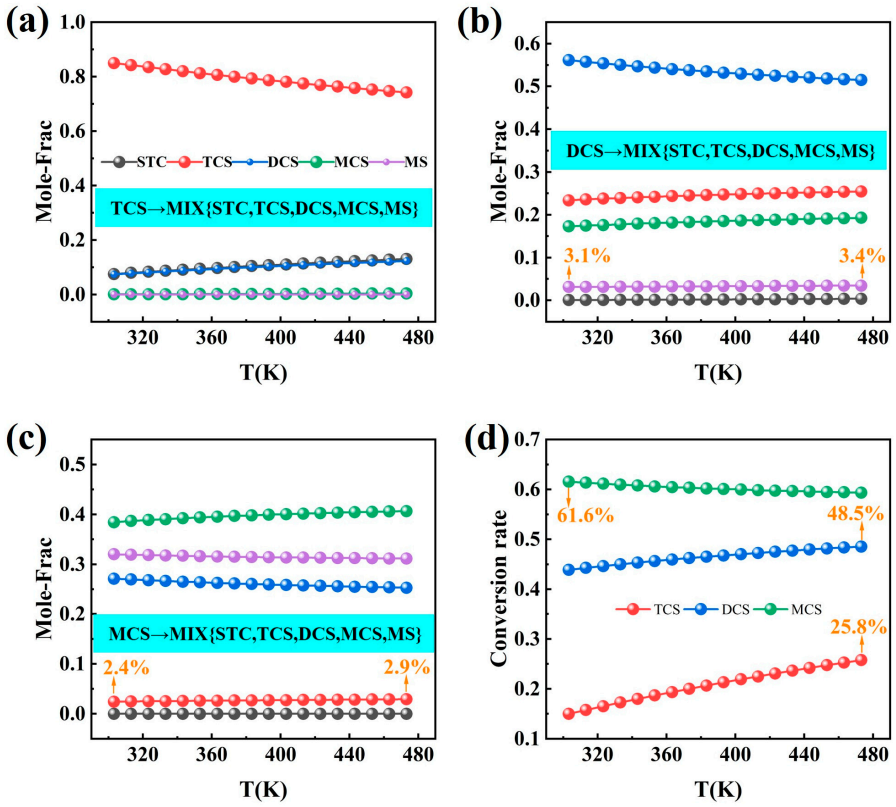


Figure 3. The molar fraction of equilibrium products and reactant conversion rate varies with reaction temperature at 303.15–473.15 K for (**a**) pure TCS, (**b**) pure DCS, (**c**) pure MCS, and (**d**) reactant conversion rates.

From Figure 3a, as the temperature rises, the molar fraction of TCS declines, while the molar fractions of DCS and STC show a consistent upward trend. The molar fractions of MCS and MS are almost zero. The conclusion drawn from this is that pure TCS, as a reactant, basically only undergoes reaction R1 and yields STC and DCS, with almost no MS. In Figure 3b, the mole fraction of DCS gradually decreases with the increase in temperature, while the mole fraction of MS remains around 3%. The mole fraction of STC is almost zero, and the mole fractions of TCS and MCS both slowly advance, but the mole fraction of TCS is always greater than that of MCS. It is obvious that pure DCS occurs in reaction R2, producing TCS and MCS. In the meantime, a portion of the generated MCS is subsequently consumed as reactants for reaction R3, generating trace amounts of MS, thereby causing a consistently lower mole fraction of MCS than TCS. Whereas TCS will not undergo further reaction, R1; therefore, no STC is produced. As illustrated in Figure 3c, the mole fraction of reactant MCS increases with ascending temperature, and the mole fractions of MS and DCS gradually decrease, but the mole fraction of DCS remains lower than that of MS. The mole fraction of STC is close to 0, while the mole fraction of TCS slowly increases from 2.4% to 2.9%. A reasonable explanation is that reactant MCS undergoes partial disproportionation through reaction R3 to form DCS and MS. The generated DCS then takes place in reaction

R2 to produce TCS. So, DCS is partially consumed, resulting in a lower mole fraction than MS. Meanwhile, the trace amount of TCS does not undergo disproportionation significantly. Figure 3d indicates that high temperature promoted the conversion of reactants TCS and DCS, slightly weakening the consumption of MCS.

2.3. Reaction Model

The kinetic model or equilibrium model [19] has been successfully applied to modeling different reaction processes with sufficient accuracy and fewer adjustable parameters. It can be implemented through the built-in model in the Aspen Plus V11 software.

2.3.1. Kinetics of TCS as a Reactant

According to Figure 3a, when TCS is the reactant, essentially only the first step of disproportionation occurs. The corresponding reaction kinetics are shown in Equations (4)–(6).

$$r_1^{TCS} = k_1^{TCS}(x_{TCS}^2 - x_{STC}x_{DCS}/K_1^{TCS}) \quad (4)$$

$$\frac{dx_{TCS}}{dt} = -2r_1^{TCS} \quad (5)$$

$$x_{DCS} = x_{STC} = \frac{1 - x_{TCS}}{2} \quad (6)$$

For reaction R1, when TCS is the reactant, where r_1^{TCS} is the reaction rate; x_{STC}, x_{TCS}, x_{DCS} are mole concentrations of STC, TCS, DCS; K_1^{TCS} is the TCS equilibrium constant; and k_1^{TCS} is the TCS reaction rate constant.

2.3.2. Kinetics of DCS as a Reactant

According to Figure 3b, when DCS serves as a reactant, all three steps of the disproportionation reaction occur. The corresponding reaction kinetics are shown in Equations (7)–(14).

$$r_1 = k_1(x_{TCS}^2 - x_{STC}x_{DCS}/K_1) \quad (7)$$

$$r_2 = k_2(x_{DCS}^2 - x_{TCS}x_{MCS}/K_2) \quad (8)$$

$$r_3 = k_3(x_{MCS}^2 - x_{DCS}x_{MS}/K_3) \quad (9)$$

$$\frac{dx_{MS}}{dt} = r_3 \quad (10)$$

$$\frac{dx_{MCS}}{dt} = r_2 - 2r_3 \quad (11)$$

$$\frac{dx_{DCS}}{dt} = r_1 - 2r_2 + r_3 \quad (12)$$

$$\frac{dx_{TCS}}{dt} = r_2 - 2r_1 \quad (13)$$

$$\frac{dx_{STC}}{dt} = r_1 \quad (14)$$

For reactions R1–R3, when DCS is the reactant, where r_i (i = 1, 2, 3) is the reaction rate; K_i (i = 1, 2, 3) is the equilibrium constant; and k_i (i = 1, 2, 3) is the reaction rate constant; x_{STC}, x_{TCS}, x_{DCS}, x_{MCS}, x_{MS} are mole concentrations of STC, TCS, DCS, MCS, MS.

2.3.3. Reaction Equilibrium Model

Compared with the kinetic model, the reaction equilibrium model is much simpler. The equilibrium constants [10] for the three reactions R1–R3, were calculated based on the

mole fractions of the equilibrium products at different temperatures using the following Equations (15)–(18).

$$K_1 = [x_{STC}][x_{DCS}]/[x_{TCS}]^2 \quad (15)$$

$$K_2 = [x_{TCS}][x_{MCS}]/[x_{DCS}]^2 \quad (16)$$

$$K_3 = [x_{DCS}][x_{MS}]/[x_{MCS}]^2 \quad (17)$$

$$lnK_i = A_i + B_i/T + C_i ln(T) \quad (18)$$

The K represents the reaction equilibrium constant, [x] is the equilibrium molar concentration of the component, T is the temperature in Kelvin, and A_i, B_i, C_i (i = 1, 2, 3) are the coefficients of the built-in balance model.

2.4. Experimental Results and Analysis

2.4.1. Experimental Scheme

The chemical reagents used in the experiment are listed in Supplementary Material Table S3. The main experimental equipment used in these studies is described in Supplementary Material Table S4. In this paper, eleven commercial resin catalysts were selected, including seven basic resins—IRA-900, A21, A100, D301, D201, D380 (-NH_2 type), and IRA-400 (-OH type)—and four acidic resins: 717, D001, A35, and IR-120. The resin was washed with deionized water and ethanol, then dried at 80 degrees for future use. The influence of various catalysts on the disproportionation reaction was studied in the intermittent device shown in Supplementary Material Figure S1. In addition, the optimal reaction conditions for the selected catalysts were also determined. The kinetic parameters and equilibrium data of the disproportionation reactions were determined using the evaluation device shown in Figure 4, ultimately establishing the theoretical conditions required for subsequent simulation and optimization of the silane process.

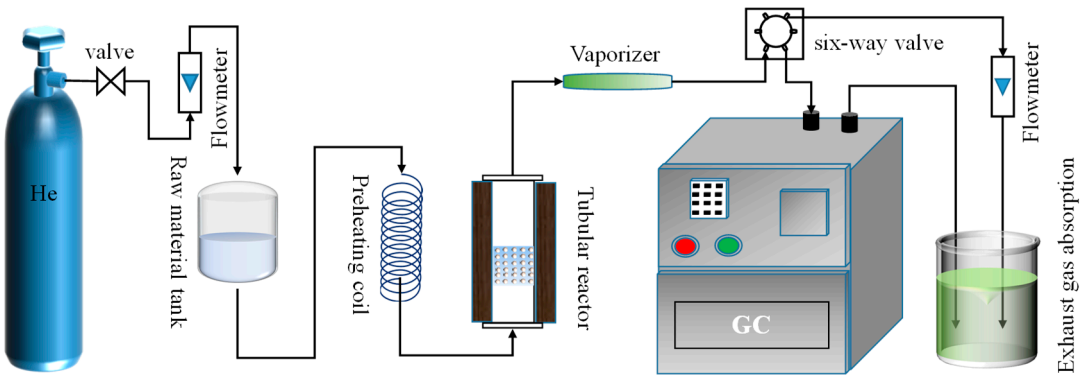


Figure 4. Schematic diagram of catalytic disproportionation reaction experiment.

The experiment was conducted in a tubular bed reactor (with a length of 450 mm and an inner diameter of 10 mm). The catalyst was placed in the middle of the reactor and supported by quartz wool. Before starting the reaction, the entire system was purged with helium for 30 min to remove water and air from the reaction system. The experiment started, and the temperatures of the preheater and the reactor were heated to the required constant values. The temperatures were set by a voltage regulator and monitored through thermocouples. Chlorosilane from the pressurized storage tank entered the reactor with the resin catalyst through the preheating section. The flow rate was monitored by the liquid level in the feed tank or the flow meter at the gas phase outlet. The reaction residence time was changed within a smaller range by altering the flow rate of the reaction stream and within a larger range by changing the bed height inside the reactor. The

effluent was evaporated and introduced into a gas chromatograph equipped with a thermal conductivity detector (TCD) for analysis. Helium was used as the carrier gas. Inside the gas chromatograph, a column with a length of 5 m and an inner diameter of 3 mm, filled with 15% DC-550/Chromo, was used for product analysis. The column temperature was maintained at 40°C, the injector temperature was set at 150°C, the detector temperature was 150°C, and the hot wire temperature was adjusted to 180°C. The identification of product types was calibrated by the retention time of standard samples and quantitatively analyzed using the area normalization method. To ensure the accuracy of the results, three repeated sampling analyses were conducted, minimizing the risk of analytical errors. The raw material tank was subjected to low-temperature insulation treatment, all pipelines were insulated to prevent heat loss, and the exhaust gas was absorbed.

2.4.2. Analysis of Reaction Conditions

Thermodynamic analysis indicates that increasing the temperature will promote the TCS disproportionation reaction. Therefore, the aim of this experimental study is to provide guidance for the application of industrial catalysts and to achieve efficient and economical production of silane. Figure 5 presents the catalytic results of different resins and simple structural characterization.

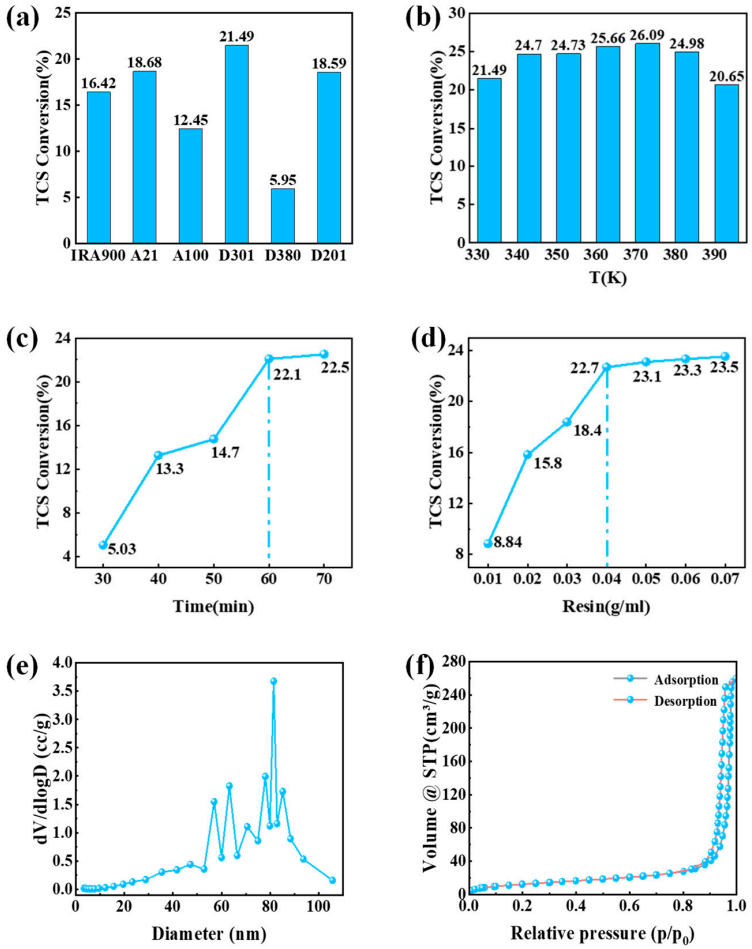


Figure 5. Trichlorosilane disproportionation reaction: (**a**) Catalytic effects of different resins (reaction time 1 h, reaction temperature 333 K, catalyst dosage 0.04 g/mL TCS); (**b**) TCS conversion rate at different temperatures (reaction time 1 h, catalyst dosage 0.04 g/mL TCS); (**c**) Effect of reaction time on TCS conversion rate (reaction temperature 343 K, catalyst dosage 0.04 g/mL TCS); (**d**) Effect of catalyst dosage on TCS conversion rate (reaction temperature 343 K, reaction time 1 h); (**e**) Pore size distribution of D301 resin; (**f**) N_2 adsorption–desorption isotherm of D301 resin.

The results show that the four acidic cation resins and the -OH type IRA-400 basic anion resin have no catalytic activity, while the other six amino resins have catalytic activity. From Figure 5a, it can be clearly seen that, except for the -NH_2 type D380 resin, the other five quaternary ammonium salt resins can significantly promote the disproportionation reaction of trichlorosilane. Among them, D301 resin has better catalytic performance, with a TCS conversion rate of 21.49%. Based on these findings, subsequent research uses D301 resin as a typical case. The influence of different reaction temperatures on the TCS conversion rate is shown in Figure 5b. It is found that increasing the reaction temperature is beneficial to the disproportionation of TCS, and the optimal conversion rate is reached at 373 K. However, further increasing the temperature will significantly decrease the conversion rate of TCS, which may be due to the destruction of the resin structure or the loss of active functional groups at high temperatures. As shown in Figure 5c, the TCS conversion rate gradually increases with the extension of the reaction time to reach equilibrium. Experimental analysis indicates that a conversion rate of 22.1% was achieved within 60 min of reaction time. Further extension of the residence time will result in a smaller increase in the TCS conversion rate, which may lead to a sharp increase in equipment operation costs. As shown in Figure 5d, the TCS conversion rate will increase with the increase in catalyst dosage, and the enhancement effect will weaken when the dosage exceeds 0.04 g/mL TCS. Subsequently, the pore size of D301 resin was analyzed. Figure 5e,f both indicate that D301 resin has a macroporous structure. Figure S2 in the Supplementary Material also shows the SEM image of D301 resin after high-temperature reaction, where high temperature causes the resin surface pores to collapse, thereby reducing the catalytic activity of the resin, which is consistent with the observed reduction in the conversion rate of the resin at 393 K. In summary, based on the experimental data, it is inferred that in the subsequent simulation, the reaction temperature of TCS should be set at 343 K, and the disproportionation residence time should be approximately 60 min to improve the economic efficiency of silane production. For each temperature of the chlorosilane disproportionation reaction, there is a corresponding time to reach the final equilibrium. Once equilibrium is established, the reaction stops. The scope of this experimental study aims to provide a reference for simulation. The dosage of the catalyst and reaction conditions in industrial applications must be optimized through systematic industrial experiments.

2.4.3. Kinetic Parameters and Chemical Equilibrium

From the distribution of the equilibrium products, it can be seen that when using TCS as the raw material, only the first step of disproportionation occurs, while when using DCS as the raw material, silane is produced. Therefore, the kinetic equation in Section 2.3 was established. Through the continuous experiment using the device shown in Figure 4, the liquid flow rate is 20 mm/min, the catalyst bed height is 100 mm, the bed diameter is 10 mm, and the kinetic data of the disproportionation reaction at different reaction temperatures, as shown in Figure 6, were obtained.

In Figure 6a–c, the reaction kinetics experiments were conducted using D301 resin with TCS as the reactant at different temperatures, and the kinetic equations were obtained. The reaction rate constants are shown in Figure 6d. With DCS as the reactant, the composition of the products over time was studied at different temperatures, as shown in Figure 6e–h, which shows the reaction rate constants of each reaction at different temperatures. In summary, increasing the temperature will promote the disproportionation of TCS and DCS. The disproportionation reaction rate of TCS is slower, while that of DCS is faster. The reaction rate constants corresponding to different reactants are shown in Supplementary Material Table S5. From Equation (18), the parameters of the built-in balance model [20] expression in the Aspen Plus software can be calculated as follows in Supplementary

Material Table S6. The subsequent modeling of the silane process has been optimized based on these parameters.

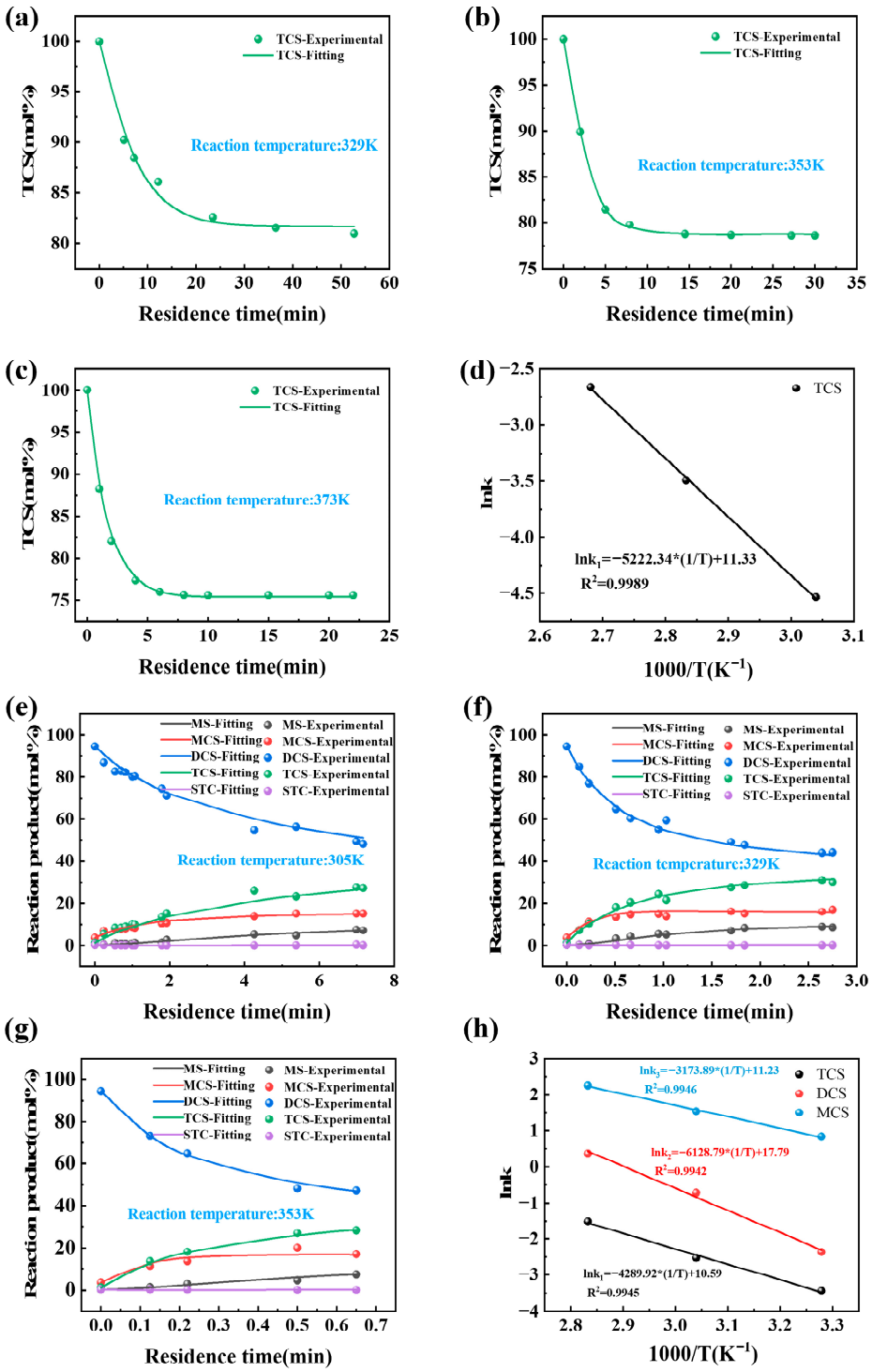


Figure 6. Effect of temperature on TCS effluent composition along with time when TCS is the reactant: (**a**) reaction temperature at 329 K, (**b**) reaction temperature at 353 K, (**c**) reaction temperature at 373 K, (**d**) the reaction temperature effect on kinetic constants; effect of temperature on effluent product composition along with time when DCS is the reactant: (**e**) reaction temperature at 305 K, (**f**) reaction temperature at 329 K, (**g**) reaction temperature at 353 K, (**h**) the temperature effect on kinetic constants.

2.5. Disproportionation Unit Design

This paper uses the Aspen Plus software to establish the process for the silane disproportionation unit shown in Figure 7. The RadFrac module was used to model four distillation columns, and the CSTR module was selected for the reactors.

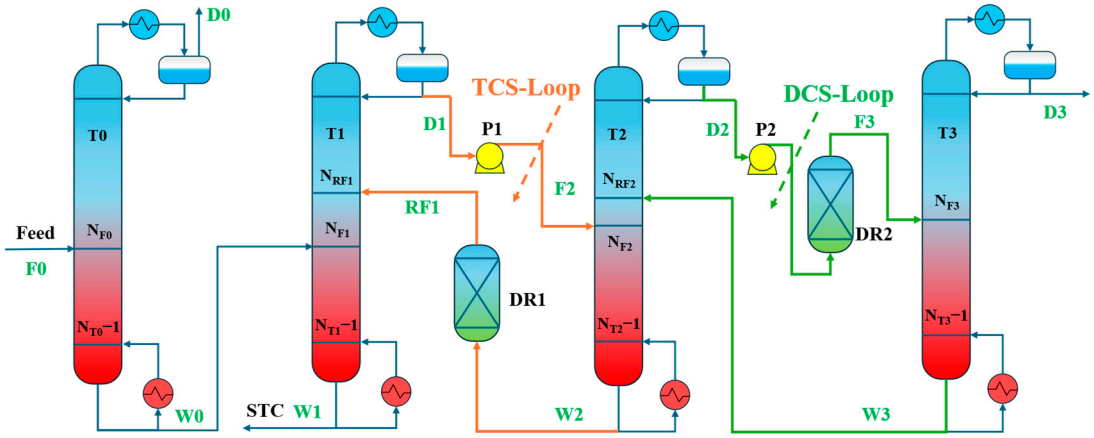


Figure 7. The flowsheet diagram of the process for the silane disproportionation unit.

According to the actual industrial data of a polysilicon factory, the feed is sourced from the hydrogenation unit at the front end, mainly a mixture of chlorosilane and light components, including 0.1 mol% H_2, 1.1 mol% DCS, 30.1 mol% TCS, 68.7 mol% STC, as given by Equations (19) and (20).

$$Si + 3SiCl_4 + 2H_2 \rightleftarrows 4SiHCl_3 \quad (19)$$

$$Si + SiCl_4 + 2H_2 \rightleftarrows 2SiH_2Cl_2 \quad (20)$$

In this process, the stripping column (T0) mainly separates the light component H_2 from the raw material, then the bottom mixture containing STC, TCS, and DCS passes through the $SiHCl_3$ separation column (T1). STC is obtained from the bottom of T1, and the TCS and DCS from the top of T1 are separated by the SiH_2Cl_2 separation column (T2). The TCS at the bottom of T2 enters the $SiHCl_3$ disproportionation reactor (DR1) mainly for reaction R1 and then returns to T1. The DCS at the top of T2 passes into the SiH_2Cl_2 disproportionation reactor (DR2) mainly for reactions R2–R3. The product stream containing MS flows into the SiH_4 separation column (T3). The MS is obtained at the top of T3, and the mixed chlorosilanes at the bottom are recycled to T2. The conventional process for the silane disproportionation unit has two reaction circulation loops, namely the TCS loop (T1-T2-DR1-T1) and the DCS loop (T2-DR2-T3-T2). Each loop has only one disproportionation reactor, which is referred to as the DR1 + DR2 process.

2.6. Multi-Objective Optimization

The optimization of the T0 column is not affected by the latter three distillation columns, with little impact on the optimization of the later distillation columns. Therefore, Figure S3 in the Supplementary Material presents optimized parameters for the stripping column T0. In the present optimization task, the variables that need optimization include the total number of stages in the three columns (N_{T1}, N_{T2}, and N_{T3}), the feed stage positions (N_{F1}, N_{F2}, and N_{F3}), as well as the feed tray locations of the circulating streams (N_{RF1} and N_{RF2}), and the reflux ratio (RR1, RR2, and RR3). This work takes the purity of the top or bottom components of the four columns as the constraint conditions (as shown in Supplementary Material Table S7) and the minimization of total annual cost (TAC) as the

objective function and proposes a sequential iterative optimization procedure, as displayed in Supplementary Material Figure S4. In order to ensure the smooth completion of the initial silane process simulation, large initial values were first given to these parameters, such as N_{T1}, N_{T2}, and N_{T3}, as well as RR1, RR2, and RR3. Taking the distillate flow rate as the variable, the purity of the top or bottom product of the column was made to meet the predetermined separation requirements.

2.7. Economic Evaluation

For the silane process, the total annual cost TAC [21,22] is adopted as the overall economic evaluation index, which can be calculated in the following Equation (21).

$$TAC = TCC/PP + TOC \tag{21}$$

where the PP stands for payback period, TCC refers to the total capital cost, and TOC represents total operating cost [23]. The investment payback period is generally set at three years. TCC mainly covers the cost of equipment such as distillation columns, condensers, reboilers, and heat exchangers. The TOC includes the consumption costs of refrigerant (cooling water or chilled water) and heat source (low, medium, and high-pressure steam). Details of the above calculations are provided in Supplementary Material Table S8.

2.8. Environmental Impact Assessment

In the current context of global energy conservation and emission reduction, the issue of carbon emissions is particularly prominent. Therefore, this work considers carbon dioxide (CO_2) emissions [24] as an indicator of environmental impact, where the use of steam as a heating medium is the source of CO_2 emissions. It can be expressed by Equation (22).

$$[CO_2]_{emissions} = C_E \times SCC \tag{22}$$

where C_E (2.493 kg/kg) and SCC correspond to the CO_2 emission conversion factor of standard coal and standard coal consumption, respectively. Furthermore, the unit steam consumption (USC) and standard coal consumption (SCC) are calculated separately [25] using Equations (23) and (24). This is an important metric in industrial production.

$$USC = \frac{Q_R \times 3600}{H_S \times \eta \times O_S} \tag{23}$$

$$SCC = \frac{Q_R \times 3600}{Q_{SC} \times \eta_{CT}} \tag{24}$$

where the USC (kg/kg) represents the unit steam consumption, Q_R (kW) represents the total duty of the reboilers, H_S (2015 kJ/kg) represents the effective enthalpy of 1.0 MPa steam, η (0.92) represents the system thermal efficiency, O_S (1260 kg/h) represents the unit output of silane, SCC (kg/h) refers the standard coal consumption, Q_{SC} (29,307 kJ/kg) refers the standard coal calorific value, η_{CT} (0.9) refers coal transmission efficiency, 3600 refers the unit conversion factor.

3. Process Design and Optimization

3.1. Design Parameters

3.1.1. Operating Pressure of Columns

Regarding the selection of the pressure of the distillation columns, it is mainly adjusted according to the temperature of the refrigerant required by the top condenser. This simulation selected two common refrigerants: one is circulating cooling water (cooling temperature 310 K), and the other is medium low temperature azeotropic refrigerant R507

(cooling temperature 233 K), which is a blend of R125 (pentafluoroethane) and R143a (trifluoroethane) with a mass ratio of 50% each, as an environmentally friendly alternative to traditional refrigerants such as R502 and R22.

Primarily, the boiling points of TCS and DCS at 101.325 kPa are 305 K and 281.35 K, respectively. The pressure of the T1 column is initially chosen at 400 kPa. At this pressure, TCS and DCS boil at 351 K and 324 K. So, the T1 column can simply be pressurized to utilize the circulating cooling water for refrigeration. As shown in Supplementary Material Figure S5a, the boiling point of pure DCS at 300 kPa is 315 K. Considering that the distillate D2 still contains a certain amount of MCS (atmospheric boiling point 242.75 K), the pressure of the T2 column was initially raised to 700 kPa in order to use the circulating cooling water. The normal pressure boiling point of pure silane is 161 K, which is very low. Therefore, as can be seen from Supplementary Material Figure S5b, in order to reduce the refrigerant duty and facilitate the use of R507, the pressure of the T3 column needs to be operated under high pressure, 2200 kPa.

3.1.2. Operating Pressure and Reaction Temperature of Reactors

The temperature of the disproportionation reactor is mainly influenced by the thermal stability of the resin catalyst, while the pressure is set to maintain the reaction in a liquid phase. Although the rate of reaching equilibrium for the gas-phase reaction is higher than that of the liquid-phase reaction, this difference is far from overcoming the significant gap in the density of the reactants. At 343 K, the mass density of liquid-phase TCS is 1238 kg/m^3, while that of the gas-phase TCS is only 15 kg/m^3. Therefore, the liquid-phase reaction system has a higher mass flux [26]. Moreover, the catalytic performance of the D301 catalyst is optimal at a temperature of 340–350 K and a reaction time of 60–80 min. The conversion rate of TCS is approximately 22%. To summarize, the initial parameters of the three distillation columns and two disproportionation reactors are presented in Table 1.

Table 1. Silane preparation process with detailed design parameters.

	Parameters					
	P/kPa	**N_T**	**N_F**	**N_{RF}**	**RR**	**D/F**
T1	400	160	120	80	1.2	0.6
T2	700	120	90	60	5	0.15
T3	2200	38	26	/	6	0.06
	P/kPa	T/K	Phase state		Residence time/min	
DR1	600	343	Liquid		60	
DR2	3800	328	Liquid		60	

3.2. Optimizations of Three Distillation Columns

The optimal parameters corresponding to the minimum TAC obtained through the sequential iterative optimization method are shown in Figures 8–10.

Figure 8a,b reveal that the optimal position (N_{F1}) for the raw material feed into the T1 column is the 92nd tray, while the outlet stream of reactor R1 returns to the T1 column through the 50th tray (N_{RF1}). It can be observed from Figure 8c that as the reflux ratio (RR1) of the T1 column increases, the top distillate D1 contains almost no STC. This is because the STC must be returned to the hydrogenation unit through the bottom of the T1 column for recycling; otherwise, it will affect the separation in the subsequent columns and the conversion rate of the reactor. More trays can achieve better separation efficiency. Figure 8d indicates that the number of trays in the T1 column simultaneously affects the purity of the top distillate D1 and the purity of the silane at the top of the T3 column. Therefore, when

the number of trays (N_{T1}) is 130, the STC content of the top distillate D1 is close to 0, and pure silane with a purity greater than 99.999% can be extracted at the top of the T3 column.

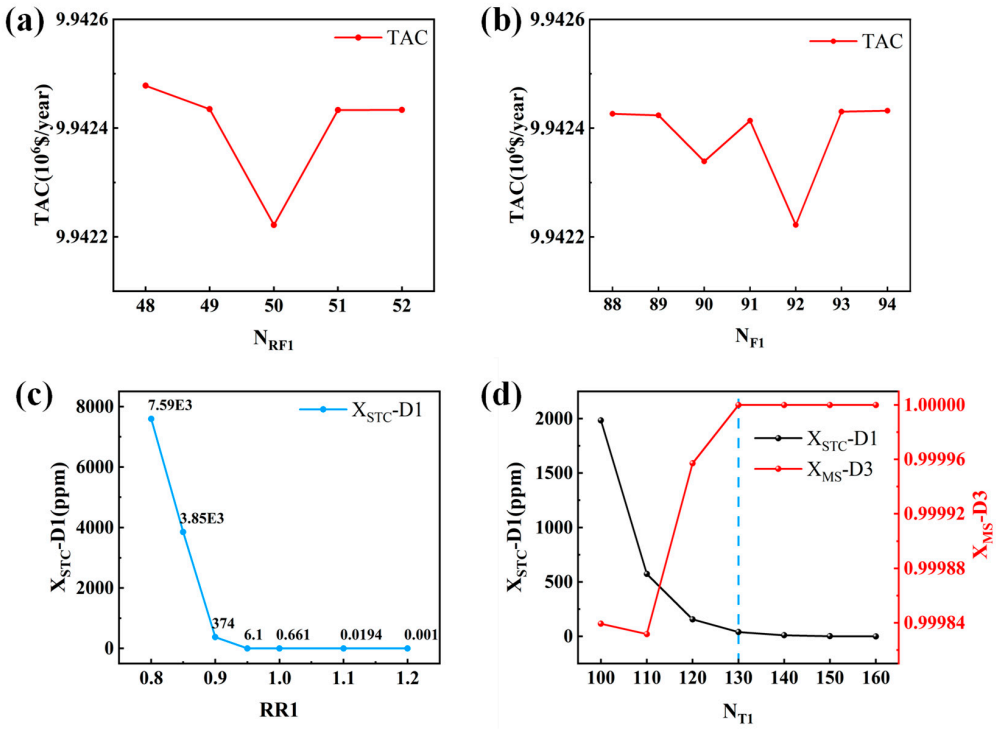


Figure 8. Optimizations of T1 column: (**a**) N_{RF1}, (**b**) N_{F1}, (**c**) RR1, and (**d**) N_{T1}.

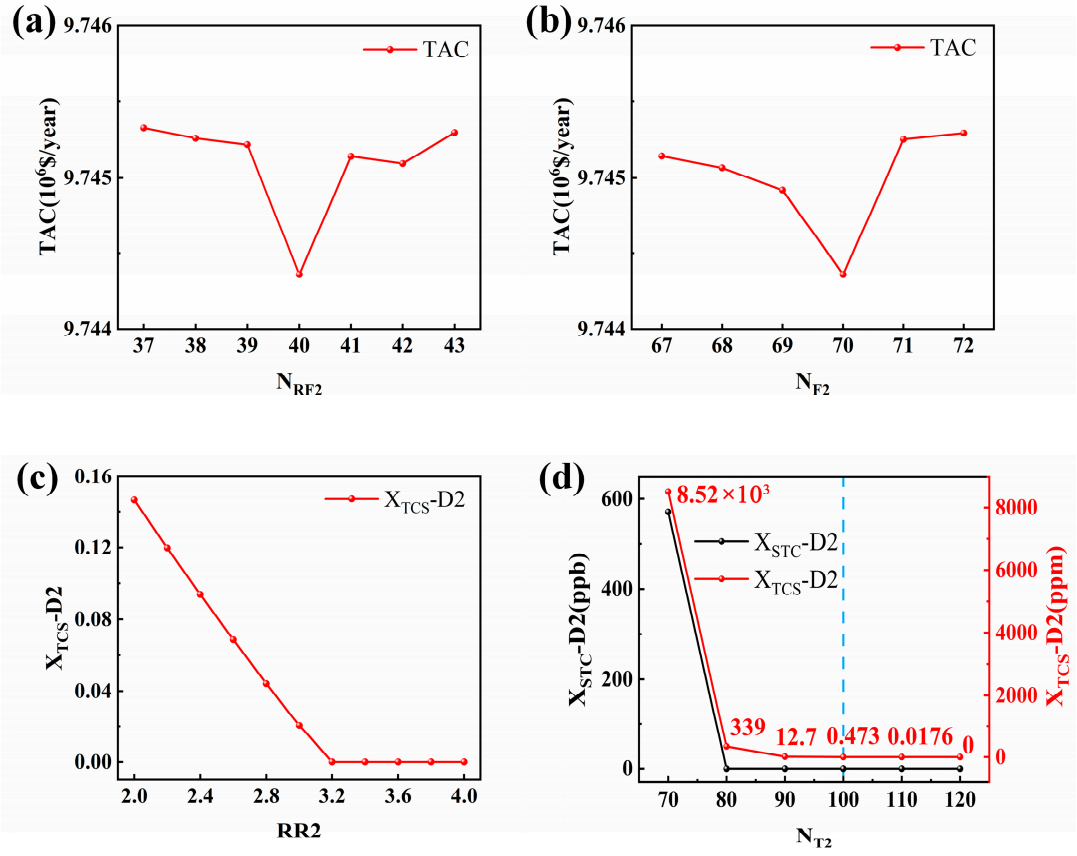


Figure 9. Optimizations of T2 column: (**a**) N_{RF2}, (**b**) N_{F2}, (**c**) RR2, and (**d**) N_{T2}.

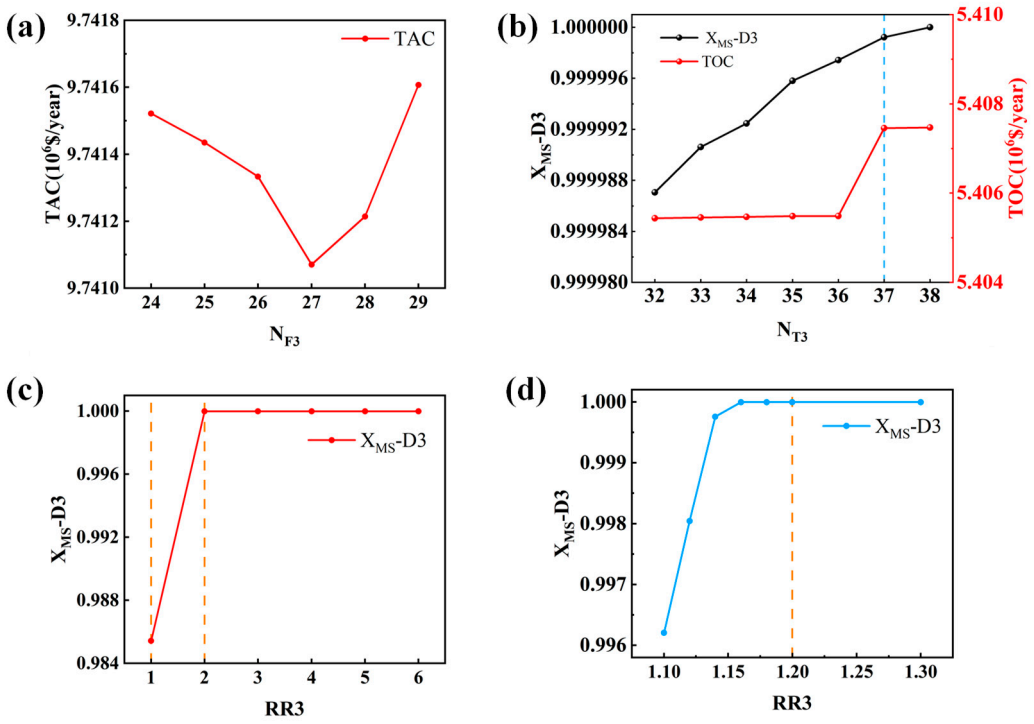


Figure 10. Optimizations of T3 column: (**a**) N_{F3}, (**b**) N_{T3}, (**c**) RR3 within the range of 1 to 6, and (**d**) RR3 within the range of 1.1 to 1.3.

From Figure 9a,b, it can be determined that the optimal feed position (N_{F2}) for column T2 is the 70th stage, and the optimal return feed position (N_{RF2}) is the 40th stage. Figure 9c illustrates that when the reflux ratio drops below 3.2, the molar fraction of TCS in the D2 significantly increases. This is not allowed to happen because a certain amount of TCS is extracted from D2 and enters reactor DR2, which will suppress the conversion rate of the DCS disproportionation reaction and also decrease the TCS content entering reactor DR1, thereby reducing the DCS production. As shown in Figure 9d, when the total number of trays is less than 80, the contents of TCS and STC in D2 rise sharply, which means that the heavy components have entered D2, and the degree of separation is not complete. Therefore, the total number of trays (N_{T2}) is set to 100 to achieve a better separation effect.

As can be seen from Figure 10a, the optimal feed position (N_{F3}) is the 27th tray. Figure 10c shows that when the reflux ratio (RR3) is less than 2, the purity of silane in the distillate D3 gradually decreases from 1 to 0.985. The reflux ratio was further refined within the range of 1–2. The optimal reflux ratio of 1.2 corresponds to a silane purity in D3 that is close to 1, as displayed in Figure 10d. A larger total number of trays is beneficial for improving the purity of silane. The conclusion drawn from Figure 10b is that when the total number of trays is greater than 36, the purity of silane is greater than 99.999%. If the number of trays is further increased, the purity of silane can be further enhanced to 1, but correspondingly, it will slightly increase operating costs. Taking all factors into consideration, the total number of column trays (N_{T3}) is set at 37.

3.3. The Silane Process Containing One DR1 and One DR2 (DR1 + DR2)

Through the optimization of the three distillation columns mentioned above, the preliminary equipment design parameters were obtained. The internal diameters of the three distillation columns were calculated using the Aspen Plus software. Firstly, all the trays were segmented based on the feed position. The internal part of the column was equipped with the Sulzer MellapakPlus 452Y type metal plate corrugated structured packing (originating from the website of Sulzer Company, Winterthur, Switzerland). The

height equivalent of a theoretical plate (HETP) was set at 0.333 m. Finally, the interactive design calculation was carried out to obtain the column diameters. Figure 11 is the flowsheet of the initially optimized silane production process.

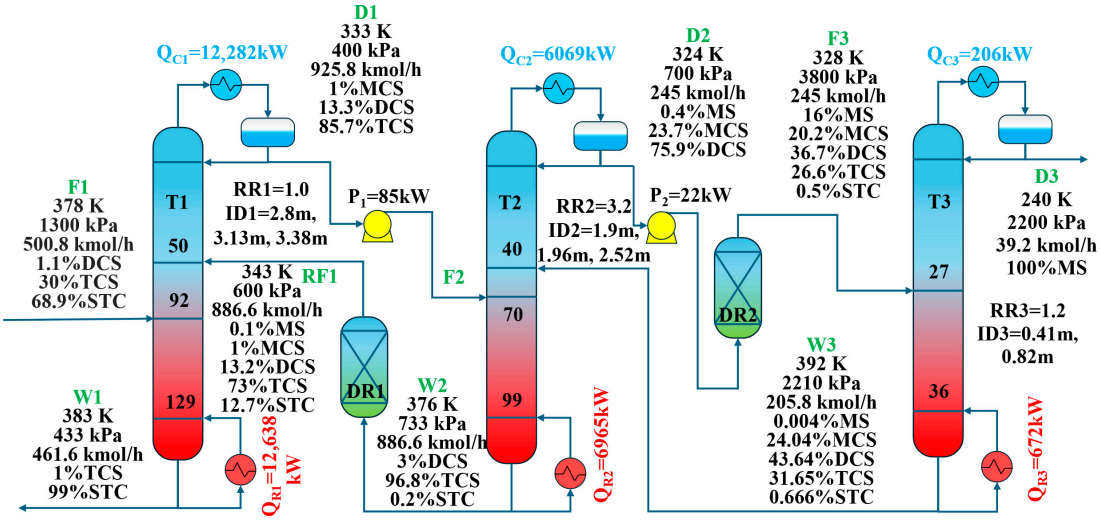


Figure 11. The flowsheet of the DR1 + DR2 process.

Compared with the actual engineering data of the inlet and outlet of the DR1 and DR2 reactors in Supplementary Material Table S9, it was found that the component contents of the stream were very close, which verified the accuracy of the model. The entire process maintains material balance. The total duty of the reboiler is 20,678 kW, and the total duty of the condenser is 18,579 kW. Furthermore, the mole flow rate of the TCS circulation loop (886.6 kmol/h) is 23 times greater than that of the MS product mole flow rate (39.2 kmol/h). The mole flow rate of the DCS circulation loop (245 kmol/h) is only 6 times that of the mole flow rate of the MS product. This is because the disproportionation conversion rate of TCS to DCS is relatively low; a distillation column is used to separate and recover more TCS for recycling back into the TCS disproportionation reactor.

In summary, the large-scale TCS recycle loop results in higher process energy consumption and larger equipment size. Therefore, this paper proposes to add an additional TCS and/or DCS disproportionation reactor in the TCS recycle loop and/or the DCS recycle loop, respectively, in order to achieve low-cost and efficient production of silane.

3.4. Novel Energy-Saving Process Design

3.4.1. The Silane Process Containing Two DR1 and One DR2 (2DR1 + DR2)

One additional TCS disproportionation reactor (+DR1) is added at the top outlet of the T1 column, forming the T1-(+DR1)-T2-DR1-T1 cycle. The flowchart shown in Figure 12 was obtained through steady-state simulation optimization.

This configuration can make beneficial changes to the compositions of the streams that make up the TCS recycle loop. Table 2 shows the changes in stream W2 leading into the first DR1, the changes in stream RF1 leading out of the first DR1, the changes in stream D1 entering the second +DR1, and the changes in stream F2 exiting the second +DR1, when the second +DR1 both is and is not present, as is the case in Figure 11 (without +DR1) and in Figure 12 (with +DR1).

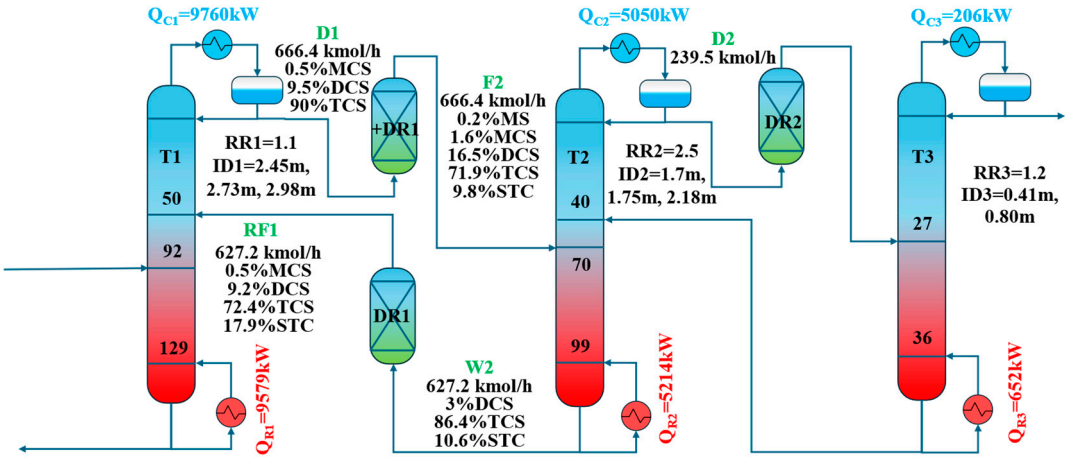


Figure 12. The flowsheet of 2DR1 + DR2 process.

Table 2. The changes in streams W2, RF1, D1, and F2.

	Figure 11-Without (+DR1)				Figure 12-with (+DR1)			
Mol%	**W2**	**RF1**	**D1**	**F2**	**W2**	**RF1**	**D1**	**F2**
MS	0.0	0.0	0.0	0.0	0.0	0.0	0.0	0.2
MCS	0.0	0.1	1.0	1.0	0.0	0.5	0.5	1.6
DCS	3.0	13.2	13.3	13.3	3.0	9.2	9.5	16.5
TCS	96.8	73.0	85.7	85.7	86.4	72.4	90	71.9
STC	0.2	12.7	0.0	0.0	10.6	17.9	0	9.8

The molar concentration of STC in stream W2 increased from 0.2% to 10.6% due to the STC produced in the second +DR1, which was separated by the T2 column and finally entered the first DR1. The TCS concentration in stream W2 decreased from 96.8% to 86.4%. This was due to the fact that the TCS in stream D1 was converted into DCS in the second +DR1. Compared with the configuration in Figure 11, when the second +DR1 was added to the process, the higher STC content and the lower TCS content resulted in a decrease in DCS concentration from 13.2% to 9.2% in stream RF1 leaving the first DR1. From a one-sided perspective, adding the second +DR1 reduced the conversion of TCS to DCS in the first DR1, which had an adverse effect. However, when considered as a combined system, the addition of the second +DR1 unexpectedly produced a very beneficial synergistic effect. In fact, because the conversion rate of TCS to DCS in each process of the TCS cycle was significantly increased, the efficiency of the silane system was greatly improved.

This brings advantages elsewhere. Due to the addition of the second +DR1, the DCS content in the feed stream F2 of the T2 column increased from 13.3% to 16.5%, the concentration of TCS reduced from 85.7% to 71.9%, and the concentration of STC increased from 0 to 9.8%. Compared with only one DR1 (Figure 11), when the TCS recycle loop contains two DR1 (Figure 12), the flow rate of the TCS recycle loop decreases from 886.6 kmol/h to 627.2 kmol/h, a reduction of 29.3%. The most direct impact is that the sizes of equipment such as T1 columns, T2 columns, condensers, reboilers, and TCS disproportionation reactors have been significantly reduced. As a result, the capital expenditure required for the construction of the silane plant has decreased.

3.4.2. The Silane Process Containing One DR1 and Two DR2 (DR1 + 2DR2)

Only an additional DCS disproportionation reactor (+DR2) is added at the bottom exit of the T3 column, and a second TCS disproportionation reactor is not included

in the TCS recycle loop, forming the T2-DR2-T3-(+DR2)-T2 cycle in the DCS recycle loop. The corresponding flowchart, as illustrated in Figure 13, was obtained through steady-state simulation.

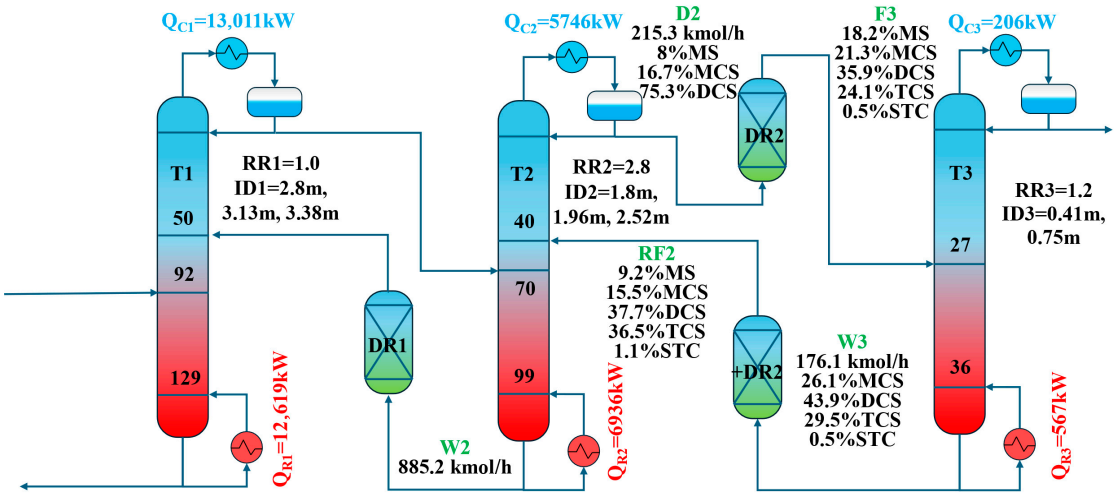


Figure 13. The flowsheet of DR1 + 2DR2 process.

By setting up two DR2s in the DCS recycle loop, beneficial changes will occur in the stream composition that constitutes the DCS circulation loop. Table 3 reflects the changes in the composition of stream D2 entering the first DR2, the changes in the composition of the stream F3 leaving the first DR2, the changes in the composition of the stream W3 leading into the second +DR2, and the changes in the composition of the stream RF2 leading out of the second +DR2, when the second +DR2 both is and is not present, as is the case in Figure 11 (+DR2 is not present) and in Figure 13 (+DR2 is present).

Table 3. The changes in streams D2, F3, W3, and RF2.

	Figure 11-Without (+DR2)				**Figure 13-with (+DR2)**			
Mol%	**D2**	**F3**	**W3**	**RF2(W3)**	**D2**	**F3**	**W3**	**RF2**
MS	0.4	16.0	0.0	0.004	8.0	18.2	0.0	9.2
MCS	23.7	20.2	24.0	24.04	16.7	21.3	26.1	15.5
DCS	75.9	36.7	43.6	43.64	75.3	35.9	43.9	37.7
TCS	0.0	20.6	31.7	31.65	0.0	24.1	29.5	36.5
STC	0.0	0.5	0.7	0.666	0.0	0.5	0.5	1.1

The incorporation of the second +DR2 significantly increased the concentration of MS in the overhead stream D2 leaving the T2 column, from 0.4% to 8.0%, which is approximately 20 times. The concentration of MS in the feed stream F3 to the T3 column rose from 16.0% to 18.2%, an increase of 13.75%. Fortunately, the concentration of MS in the feed stream RF2 flowing out from the second +DR2 to the T2 column increased from 0.004% to 9.2%, a significant increase of over 2000 times.

Compared with Figure 11, the configuration shown in Figure 13 reduces the flow rate of the DCS recycle loop from 245 kmol/h to 215.3 kmol/h, representing a 12% reduction.

Consequently, the condenser duty of the T2 column and the reboiler duty of the T3 column both decreased, and the sizes of the first DCS disproportionation reactor DR2 and the T3 column also reduced, thereby saving energy costs and equipment investment.

3.4.3. The Silane Process Containing Two DR1 and Two DR2 (2DR1 + 2DR2)

When both the second +DR1 and the second +DR2 are added simultaneously, this dual configuration, as illustrated in Figure 14, can combine the benefits of the individual configurations. That is to say, Figure 14 can obtain the additional +DR1 advantages shown in Figure 12 and the additional +DR2 advantages shown in Figure 13.

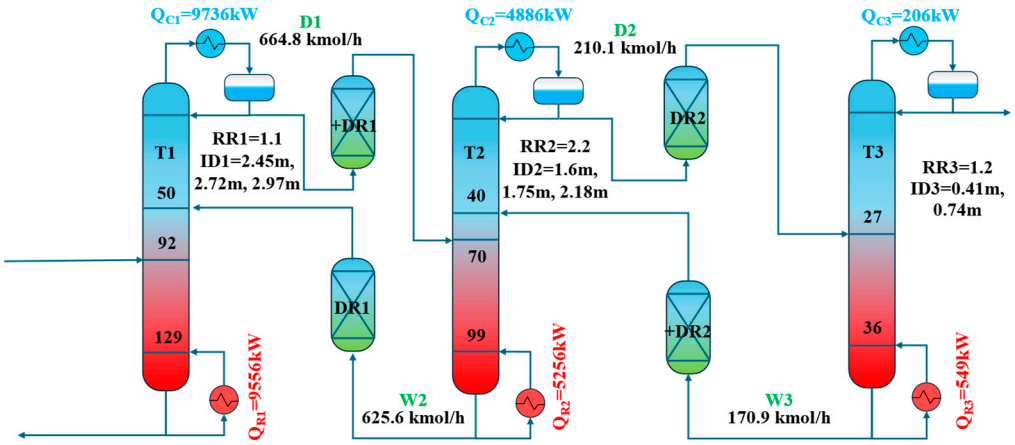


Figure 14. The flowsheet of 2DR1 + 2DR2 process.

Compared with the original process shown in Figure 11, the configuration depicted in Figure 14, which adds one TCS reactor and one DCS reactor, respectively, brings about significant economic advantages. The sizes of all the equipment used in the MS production process have been reduced, and the loads of the condensers and reboilers in all the distillation columns have been decreased.

In addition, without adding any additional reactors or other equipment, this paper further proposes an energy-saving strategy for the thermal integration of distillation columns in the following sections.

3.4.4. Heat Integration Assisted DR1 + DR2 Process (HI + DR1 + DR2)

Multi-effect heat integration significantly reduces the high energy consumption of the distillation process through the energy integration among the distillation columns. The latent heat of condensation from the top steam of the previous distillation column serves as the heat source for the reboiler of the subsequent distillation column, thereby achieving multi-level utilization of thermal energy.

The condenser duty of the T1 column is the highest, and the composition at the top of the T1 column is similar to that at the bottom of the T2 column and T3 column. Therefore, the steam from the top of the T1 column is used as the heating source for the reboilers of the other columns. In order to ensure sufficient heat transfer temperature difference between the distillation columns, the minimum heat transfer temperature difference should be controlled to be no less than 10 K. The pressure of the T0 column is controlled at 470 kPa, and that of the T3 column is maintained at 2200 kPa. Figure S6 in the Supplementary Material shows the temperature coupling relationship between the four distillation columns when the T1 column and the T2 column are at different pressures. In order to maximize the utilization of energy, it is necessary to adjust the pressure of the T1 and T2 columns so that the high-temperature gas phase at the top of the T1 column can simultaneously heat the reboilers of the T0, T2, and T3 columns. The pressure of the T1 column needs to be no less than 1400 kPa, and the pressure of the T2 column is no more than 1000 kPa.

The total duty (Q_{Total}), heat integration duty (Q_{HI}), heat integration efficiency (η), and heat integration duty difference ($\triangle Q_{HI}$) are calculated, respectively, using the following Equations (25)–(28).

$$Q_{Total} = \sum_{i=0}^{3} (|Q_{Ci}| + Q_{Ri}) \quad (25)$$

$$Q_{HI} = |Q_{C1}| - Q_{R0} - Q_{R2} - Q_{R3} + Q_{R1} + |Q_{C0} + Q_{C2} + Q_{C3}| \quad (26)$$

$$\eta = \frac{Q_{Total} - Q_{HI}}{Q_{Total}} \times 100\% \quad (27)$$

$$\Delta Q_{HI} = |Q_{C1}| - Q_{R0} - Q_{R2} - Q_{R3} \quad (28)$$

Q_{Ci} (kW) represents the condenser duty, and Q_{Ri} (kW) is the reboiler duty (i = 0, 1, 2, 3).

Therefore, the heat integration effect under different conditions is shown in Figure 15. First of all, Figure 15a indicates that when the pressure of the T2 column is 700 kPa, continuously increasing the pressure of the T1 column to 1400 kPa achieves the maximum heat integration efficiency of 37.35%. Further increasing the pressure leads to a decrease in heat integration efficiency because at this point, the reboiler heat duty of the T1 column is relatively large, resulting in a greater total duty. So, the pressure of the T1 column is set to 1400 kPa. As can be seen from Figure 15b, gradually increasing the pressure of the T2 column to 1000 kPa also increases the heat integration efficiency. The maximum thermal integration efficiency is 39.05%. When the pressure of the T2 column exceeds 1000 kPa, the minimum heat transfer temperature difference will be less than 10 K, as shown in Supplementary Material Figure S6. In order to achieve complete utilization of energy, Figure 15c shows that reducing the DCS content in W2 can make the heat integration duty difference gradually approach 0. This is because the T2 column requires a larger reflux ratio to meet the separation effect, and correspondingly, the reboiler duty of the T2 column continues to increase. When the molar content of DCS is within the range of 0.0008 to 0.0004, the best heat integration effect can be achieved. In Figure 15d, when the content of DCS is controlled at 0.0006 and the reflux ratio of the T2 column is 5.68, the corresponding heat integration efficiency is the best, which is 45.46%.

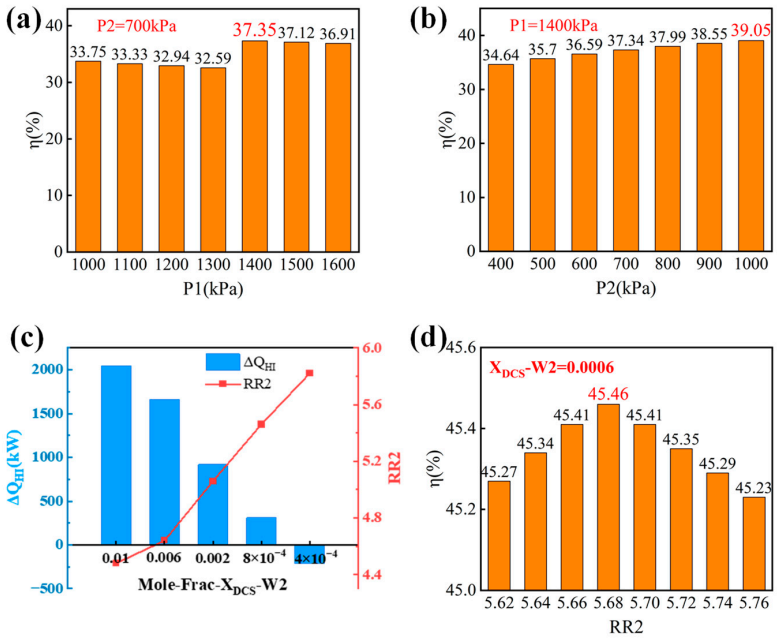


Figure 15. The heat integration effect: (**a**) different pressures of T1 column, (**b**) different pressures of T2 column, (**c**) different DCS contents of W2, and (**d**) different RR2.

In addition, the high-temperature stream W1 at the bottom of T1 column can be used to heat the stream RF1 at the outlet of DR1, maintaining a temperature difference of 10 K between the hot outlet and the cold inlet. This significantly reduces the reboiler duty of the T1 column. The cooled STC can be recycled and sent to the cold hydrogenation unit. When adopting the four-column heat integration strategy, the schematic diagram of the HI + DR1 + DR2 process flow is shown in Figure 16. The total duty of this process is the sum of the condenser duties of T0, T2, and T3 columns and the reboiler duty of T1 column, which is 21,478 kW. Compared with the DR1 + DR2 process shown in Figure 11, the total duty has been significantly reduced by 45.3%.

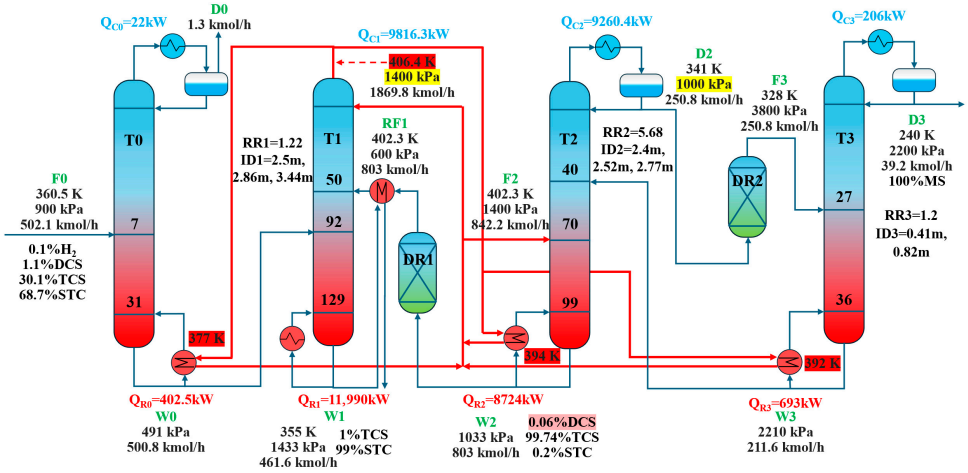


Figure 16. The flowsheet of HI + DR1 + DR2 process.

3.4.5. Heat Integration Assisted 2DR1 + 2DR2 Process (HI + 2DR1 + 2DR2)

Based on the previous research conclusions, it is quite straightforward to apply the heat integration strategy to the 2DR1 + 2DR2 process configuration shown in Figure 14 and obtain the HI + 2DR1 + 2DR2 process as described in Figure 17, thereby achieving the maximum utilization of energy.

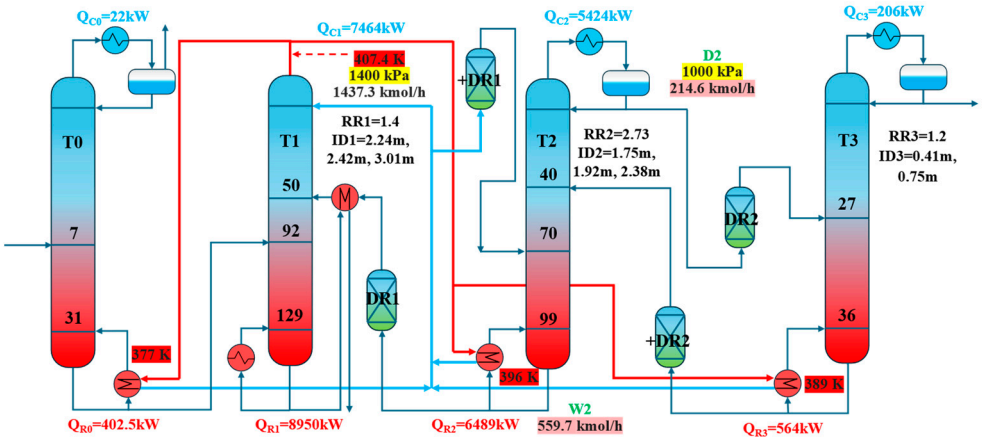


Figure 17. The flowsheet of HI + 2DR1 + 2DR2 process.

The total energy consumption of the process configuration shown in Figure 17 is 14,602 kw, which is 32.1% lower than that of the configuration in Figure 16 and 52.3% less than that of the configuration in Figure 14. More importantly, compared to the original DR1 + DR2 process illustrated in Figure 11, the energy consumption has been greatly reduced by 62.8%. Meanwhile, the flow rate of the TCS recycle loop decreased from 886.6 kmol/h to 559.7 kmol/h, representing a reduction of 36.87%.

3.5. Process Performance Evaluation and Analysis

The condenser duty (Q_C), reboiler duty (Q_R), total duty (Q_{Total}), recycle loop flow rate for these six configurations were compared, as shown in Figure 18. Compared with the conventional DR1 + DR2 process, all five intensified processes have saved energy consumption. Among them, the HI + 2DR1 + 2DR2 process is the most efficient. From Figure 18a,b, the HI + 2DR1 + 2DR2 process simultaneously saves the energy consumption of the reboilers in the T0, T2, and T3 columns and the duty of the condenser in the T1 column. Figure 18c shows that the condenser duty has decreased by 69.58%, the reboiler duty has reduced by 56.72%, and the total energy consumption of the process has significantly decreased by 62.8%. In addition, Figure 18d illustrates that the TCS recycle loop flow has reduced by 36.87%, and the DCS recycle loop flow has decreased by 12.41%.

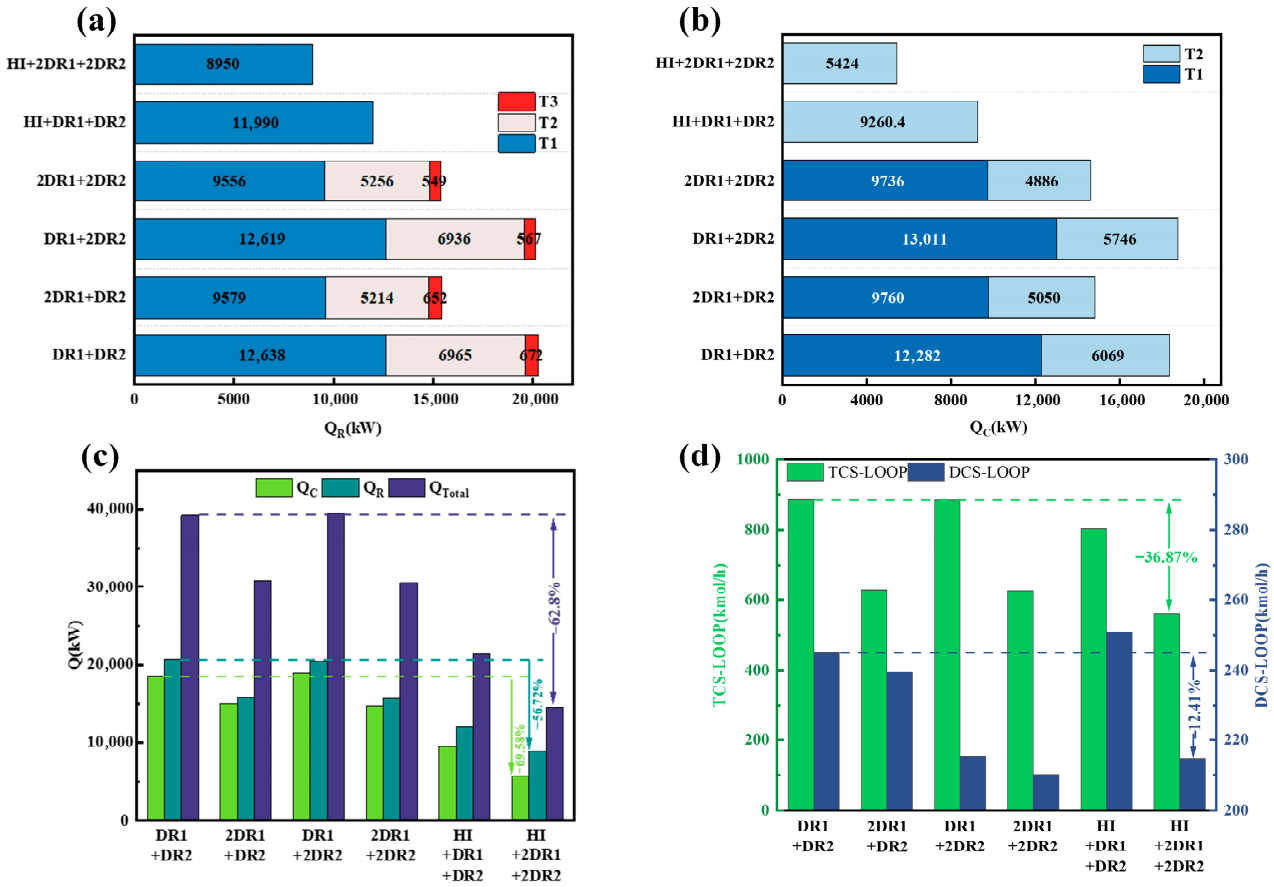


Figure 18. Comparison: (**a**) reboiler duty, (**b**) condenser duty, (**c**) total duty, (**d**) recycle loop flow rate.

Furthermore, the production costs and gas emissions are significant economic and environmental issues that must be addressed in the chemical production process. The unit steam consumption (USC), standard coal consumption (SCC), and CO_2 emissions for each process are shown in Figure 19. As stated in Equations (22)–(24), the USC, SCC, and CO_2 emissions are directly related to the reboiler duty. The HI + 2DR1 + 2DR2 configuration shows a 56.72% reduction in reboiler duty relative to the DR1 + DR2 configuration, which directly correlates with superior economic and environmental performance. As demonstrated in Figure 19a,b, this energy efficiency advantage manifests as a 56.72% decrease in USC, SCC, and CO_2 emissions for the HI + 2DR1 + 2DR2 process compared to the DR1 + DR2 process, fundamentally attributable to the more energy-consuming operation mode of the DR1 + DR2 process. The USC is only 13.8 kg steam/kg SiH_4. Based on an annual production time of 8000 h, it can save 12,805 tons of standard coal annually.

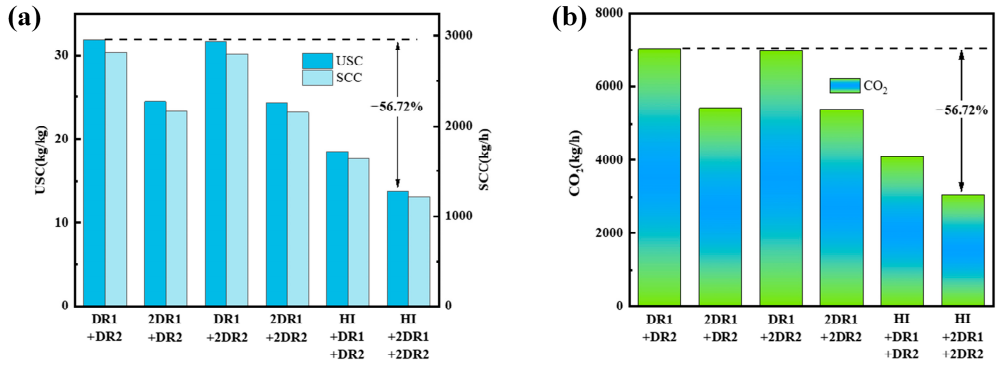


Figure 19. Comparison: (**a**) unit steam consumption, standard coal consumption, (**b**) CO_2 emissions.

Therefore, by simply adding two simple pieces of equipment, one TCS disproportionation reactor and one DCS disproportionation reactor, and carrying out an energy heat integration design, it is easy to retrofit the existing silane plants and reduce the operating duty of the existing distillation columns, with attendant benefits in energy savings.

4. Conclusions

In this paper, the thermodynamic principles of the disproportionation reaction were first analyzed. Subsequently, the performance of the resin catalyst was compared, and the optimal reaction conditions were determined. The experimental results show that the catalytic activity of D301 resin is the highest. At 343 K, the conversion rate of TCS can reach 24.7%. The reaction rate constant and equilibrium constant were obtained through kinetic experiments, providing data references for subsequent simulations.

This paper presents an advanced fixed-bed process with an annual ten-thousand-ton class production capacity, providing a sustainable solution for the low-cost production of high-purity silane. Through steady-state simulation and multi-scale optimization, the optimal operating parameters of the conventional DR1 + DR2 process were obtained. First, three optimal process configurations were proposed, including adding additional disproportionation reactors in the TCS recycle loop and/or the DCS recycle loop, namely the 2DR1 + DR2 process, the DR1 + 2DR2 process, and the 2DR1 + 2DR2 process. Furthermore, based on the configuration of the 2DR1 + 2DR2 process, a novel HI + 2DR1 + 2DR2 process combined with four-column heat integration technology was developed, enabling energy coupling between all distillation columns within the production unit while saving both condensation duty and heating duty. In comparison to the initial DR1 + DR2 process, the HI + 2DR1 + 2DR2 process was the most economical and environmentally-friendly process and could reduce total production duty by 62.8%, TCS recycle loop flow rate by 36.87%, DCS recycle loop flow rate by 12.41%, and CO_2 emissions by 56.72%. And the unit steam consumption of silane was only 13.8 kg steam/kg SiH_4, with notable carbon emission reduction potential and economic benefits.

Most importantly, this configuration is easy to retrofit to the existing process of silane plants. By connecting it in series with the cold hydrogenation unit in the traditional improved Siemens process, continuous production from metallurgical-grade silicon to electronic-grade silane can be achieved, and the complete recycling and utilization of by-products can also be realized. This modular design provides a theoretical basis for the expansion and implementation of large-scale industrial installations.

Supplementary Materials: The following supporting information can be downloaded at: https://www.mdpi.com/article/10.3390/separations13040127/s1, Figure S1. The simple apparatus and process for the trichlorosilane disproportionation experiment. Figure S2. SEM image of D301 resin after high-temperature reaction. (a) 500 μm scale, (b) 5 μm scale. Figure S3. The optimized parameters

of stripping column T0. Figure S4. The sequential iterative optimization procedure. Figure S5. The boiling points of substances under different pressures (a) DCS, (b) MS. Figure S6. The temperature coupling relationship (a) change in pressure of T1 column, (b) change in pressure of T2 column. Figure S7. The TG-DTG curves of D301 resin. Table S1. The molecular weights and boiling points of components. Table S2. Thermodynamic parameters of related substances under standard state. Table S3. Experimental materials and reagents. Table S4. Experimental instruments. Table S5. Disproportionation reaction rate constant and equilibrium constant. Table S6. Parameters of the built-in balance model. Table S7. The constraint conditions of four columns. Table S8. Equipment size and economic calculation. Table S9. Comparison of engineering data and simulation results for the fixed-bed process.

Author Contributions: Conceptualization, Q.G. and G.H.; methodology, Q.G.; software, G.H.; validation, Q.G., T.L. and G.H.; formal analysis, T.L.; investigation, T.L.; resources, G.H.; data curation, Q.G.; writing—original draft preparation, Q.G.; writing—review and editing, Q.G.; visualization, T.L.; supervision, G.H.; project administration, G.H.; funding acquisition, G.H. All authors have read and agreed to the published version of the manuscript.

Funding: This research received no external funding.

Data Availability Statement: Data is contained within the article or Supplementary Material.

Conflicts of Interest: Author Tianshi Lan was employed by the company GCL Technology Holdings Limited. The remaining authors declare that the research was conducted in the absence of any commercial or financial relationships that could be construed as a potential conflict of interest.

References

1. Yoon, D.; Shin, H.; Oh, S.; Jo, C.; Lee, K.; Jung, S.; Ko, D.-H. Characteristics of high-order silane based Si and SiGe epitaxial growth under 600 °C. *J. Cryst. Growth* **2024**, *632*, 127642. [CrossRef]
2. Xie, M.; Ruan, J.; Bai, W.; Qiao, Q.; Bai, L.; Zhang, J.; Li, H.; Lv, F.; Fu, H. Pollutant payback time and environmental impact of Chinese multi-crystalline photovoltaic production based on life cycle assessment. *J. Clean. Prod.* **2018**, *184*, 648–659. [CrossRef]
3. Jiang, Z.-J.; Luo, Z.-H.; Guo, J.-X.; Du, Y.-F.; Jiang, F.; Shen, N.-L.; Wang, T.; Liu, X.; Huang, J.; Chen, W.-H.; et al. Thermal safety overview of silicon-carbon anode in lithium-ion batteries: Key parameters in determining the reactivity. *Particuology* **2025**, *100*, 178–185. [CrossRef]
4. Zhang, P.; Duan, J.; Chen, G.; Li, J.; Wang, W. Production of polycrystalline silicon from silane pyrolysis: A review of fines formation. *Sol. Energy* **2018**, *175*, 44–53. [CrossRef]
5. Ramírez-Márquez, C.; Otero, M.V.; Vázquez-Castillo, J.A.; Martín, M.; Segovia-Hernández, J.G. Process design and intensification for the production of solar grade silicon. *J. Clean. Prod.* **2018**, *170*, 1579–1593. [CrossRef]
6. Bye, G.; Ceccaroli, B. Solar grade silicon: Technology status and industrial trends. *Sol. Energy Mater. Sol. Cells* **2014**, *130*, 634–646. [CrossRef]
7. Ceccaroli, B.; Lohne, O.; Øvrelid, E.J. New advances in polysilicon processes correlating feedstock properties and good crystal and wafer performances. *Phys. Status Solidi C* **2012**, *9*, 2062–2070. [CrossRef]
8. Müller, A.; Ghosh, M.; Sonnenschein, R.; Woditsch, P. Silicon for photovoltaic applications. *Mater. Sci. Eng. B* **2006**, *134*, 257–262. [CrossRef]
9. Vorotyntsev, A.V.; Petukhov, A.N.; Razov, E.N.; Makarov, D.A.; Vorotyntsev, V.M. Catalytic Activity of Amberlyst A-21 in the Disproportionation of Trichlorosilane at Critical Temperatures. *Catal. Ind.* **2019**, *10*, 263–269. [CrossRef]
10. Shuaishuai, S.; Guoqiang, H. Simulation of Reactive Distillation Process for Monosilane Production via Redistribution of Trichlorosilane. *Chin. J. Chem. Eng.* **2014**, *22*, 287–293. [CrossRef]
11. Huang, K.; Yuan, Y.; Zang, X.; Chen, H.; Zhang, L.; Qian, X.; Wang, S. Controllability Evaluation for Reactive Distillation Columns with Multiple Reactive Sections Disproportionating Trichlorosilane to Silane. *Ind. Eng. Chem. Res.* **2018**, *57*, 1102–1108. [CrossRef]
12. Lee, H.-Y.; Chen, Y.-Y.; Eiamsuttitam, P.; Alcántara-Avila, J.R. Comparison of optimization methods for the design and control of reactive distillation with inter condensers. *Comput. Chem. Eng.* **2022**, *164*, 107871. [CrossRef]
13. Li, K.Y.; Huang, C.D. Redistribution Reaction of Trichlorosilane in a Fixed-Bed Reactor. *Ind. Eng. Chem. Res.* **1988**, *27*, 1600–1606. [CrossRef]
14. Medina-Herrera, N.; Tututi-Avila, S.; Jiménez-Gutiérrez, A.; Segovia-Hernández, J.G. Optimal design of a multi-product reactive distillation system for silanes production. *Comput. Chem. Eng.* **2017**, *105*, 132–141. [CrossRef]

15. Zhang, Q.; Geng, Q.; Huang, G. Investigation into economically viable reactive distillation assisted trichlorosilane disproportionation to produces silane. *Sep. Purif. Technol.* **2025**, *368*, 132983. [CrossRef]
16. Mathias, P.M.; Copeman, T.W. Extension of the Peng-Robinson equation of state to complex mixtures: Evaluation of the various forms of the local composition concept. *Fluid Phase Equilibria* **1983**, *13*, 91–108. [CrossRef]
17. Nelson, W.M.; Naidoo, P.; Ramjugernath, D. Phase equilibrium data for potentially hazardous binary mixtures involving dichlorosilane, trichlorosilane and silicon-tetrachloride. *J. Chem. Thermodyn.* **2015**, *91*, 420–426. [CrossRef]
18. Hunt, L.P.; Sirtl, E. A Thorough Thermodynamic Evaluation of the Silicon-Hydrogen-Chlorine System. *J. Electrochem. Soc.* **1972**, *119*, 1741–1745. [CrossRef]
19. Santaella, M.A.; Gutiérrez, M.F.; Orjuela, A. Tributyl citrate production via reactive distillation: Model reconciliation, optimization, scale up and sustainability indicators. *Chem. Eng. J.* **2022**, *433*, 133199. [CrossRef]
20. Bi, R.; Yan, K.; Yang, H.; Tan, X.; Xiang, S. Simulation and optimization of the thermally coupled reactive distillation column for producing toluene diisocynate. *AIChE J.* **2022**, *69*, e17648. [CrossRef]
21. Duanmu, F.; Sorensen, E. Optimal design of reduced vapor transfer dividing wall structures with and without heat integration. *AIChE J.* **2024**, *70*, e18572. [CrossRef]
22. Zhang, Y.; Zhou, M.; Wang, Y.; Zhu, Z.; Wang, Y.; Cui, P.; Qi, J.; Yang, J.; Wang, F. Efficient separation in n-butyl ether production process from computational thermodynamics to process intensification. *AIChE J.* **2024**, *70*, e18492. [CrossRef]
23. Yang, A.; Shen, W.; Wei, S.A.; Dong, L.; Li, J.; Gerbaud, V. Design and control of pressure-swing distillation for separating ternary systems with three binary minimum azeotropes. *AIChE J.* **2019**, *65*, 1281–1293. [CrossRef]
24. Sun, Q.; Zhai, J.; Peng, Z.; Li, J.; Xie, H.; Liang, H.; Xu, W.; Zhang, J. Multi-objective optimisation and energy-saving design of pressure-swing extractive distillation for separating ethanol/acetonitrile/water azeotropic system. *Chem. Eng. Sci.* **2025**, *305*, 121131. [CrossRef]
25. Yu, A.; Ye, Q.; Li, J.; Wang, Y.; Rui, Q. Energy-saving improvement of heat integration and heat pump for separating multi-azeotropes mixture via novel pressure swing distillation. *Chem. Eng. Sci.* **2023**, *282*, 119239. [CrossRef]
26. Breneman, W.C.; Mui, J.Y.P. Low cost silicon solar array project. Task 1: Establishment of the feasibility of a process capable of low cost, high volume production of silane, SiH4. In *Annual Report Union Carbide Corp*; Union Carbide Corporation: Sistersville, WV, USA, 2019.

Disclaimer/Publisher's Note: The statements, opinions and data contained in all publications are solely those of the individual author(s) and contributor(s) and not of MDPI and/or the editor(s). MDPI and/or the editor(s) disclaim responsibility for any injury to people or property resulting from any ideas, methods, instructions or products referred to in the content.